Pathways to exo-world discovery with fluidic space-assembled telescopes

Enrico Biancalani,[1] **Eduardo Bendek**,[2] **Kevin Wagner**,[3] **Edward Balaban**,[2] **& the FLUTE Team**

[1] UMd + NASA GSFC (via CRESST II) | [2] NASA ARC | [3] U of A

From Galileo to Fluidic Telescopes

The diameter of optical telescopes has been increasing roughly exponentially since their conception in 1608. This trend began with ground-based refractors and continued with ground-based reflectors, which sag less under gravity, since ~1900. In the second half of the 1900s, while mirror tessellation started sustaining the growth of ground-based reflectors, the first space-borne telescopes took off. Nowadays, the extremely-large telescopes under construction are challenging the limits of what is practicable on Earth, while the projected space-borne branch appears to be plateauing after JWST. Space-assembled fluidic telescopes, alias FLUTEs, can offer a solution to this scalability problem.

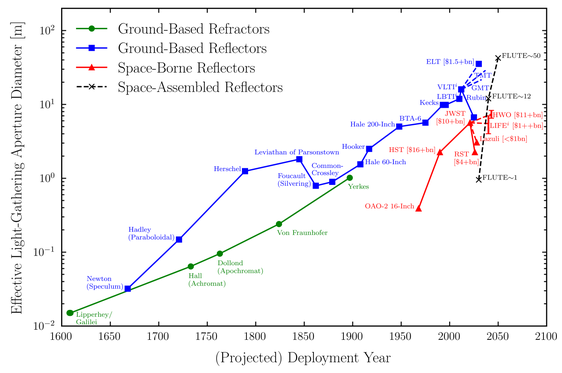

Fig. 1: Graph showing the macro-evolution of optical telescopes.

Furthermore, FLUTE's approach to in-space optics assembly may also be well suited to unlocking and streamlining the reproducibility, at a lower cost, of already-developed resource-intensive space telescopes, thus overcoming the oversubscription problem that plagues space-borne telescopes like HST, JWST, and the just-launched Roman. Although its cornerstone will be community-defined surveys, Roman's 1,200-hour Cycle 1 is already oversubscribed with a ratio of ~12:1, according to the *Roman Science Operations Center Newsletter* (May 2026).

Fig. 2 (a): Oversubscription ratio of HST, over its lifetime.

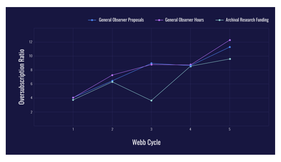

Fig. 2 (b): Oversubscription ratio of JWST, over its lifetime.

In April 2022, the first lens was created in outer space, aboard the International Space Station (ISS), via "fluidic shaping": this core scale-invariant technology underpins FLUTE and could help tackle both the scalability and oversubscription problems.

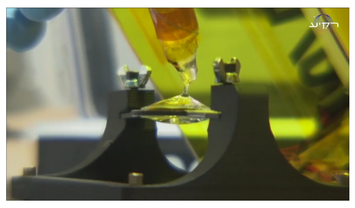

Fig. 3: Frame of the video that displays the first lens fabricated in outer space, aboard the ISS, thanks to fluidic shaping, in 2022; credits to the Bercovici Fluidic Technologies Lab.

Overall, both refractive and reflective optical components can be constructed by pinning an optical liquid to a geometrical boundary and controlling the volume of injected liquid. FLUTE's optical assembly is currently envisioned with a continuous fluidic primary mirror and an optical aberration corrector in front of it.

See Biancalani+2025 for a preliminary optical architecture trade-off framework, as well as preliminary optical designs of FLUTE-1 and FLUTE-50—both with aspherical primary mirrors, building upon the spherical designs in the Biancalani+2025 AAS-245 iPoster. For an updated optical design of FLUTE-1, see Bendek+2026 presented at SPIE AT+I.

Hereafter, a comparison of preliminary 1-μm-diffraction-limited FLUTE-1 designs, with a spherical (FLUTE-1-S, below) and with an aspherical (FLUTE-1-A, below) primary. The analysis is performed in *Ansys Zemax OpticStudio* and with the open-source software suite Photon Simulator (*PhoSim*), which enables the early holistic prototyping of digital twin observatories via Monte-Carlo-based photo-/electronic simulations.

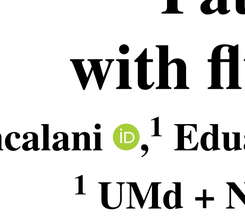

Fig. 4 (a): *Zemax OpticStudio* FLUTE-1-S's FFT 1-μm PSF.

Fig. 4 (b): Optical design of FLUTE-1-S, in *PhoSim*.

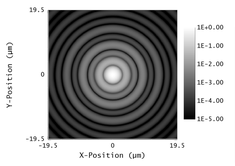

Fig. 5 (a): *Zemax OpticStudio* FLUTE-1-A's FFT 1-μm PSF.

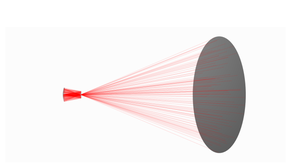

Fig. 5 (b): Optical design of FLUTE-1-A, in *PhoSim*.

Notice that the design in **Fig. 4 (b)** has a spherical aberration corrector with three mirrors and four reflections. The corrector in **Fig. 5 (b)** is more compact, with only two mirrors and two reflections, thanks to the introduction of an ellipsoidal primary mirror in our architecture trades. On the other hand, the longer effective focal length in **Fig. 4 (b)** is required by the fact that, given the same primary-mirror diameter, the Seidel spherical aberration scales with the inverse cube of the optical system's focal ratio. These versions of FLUTE-1 allow for the Nyquist sampling of the PSF's core at 1 μm by an image-plane detector with the typical pixel pitch of modern smartphone cameras.

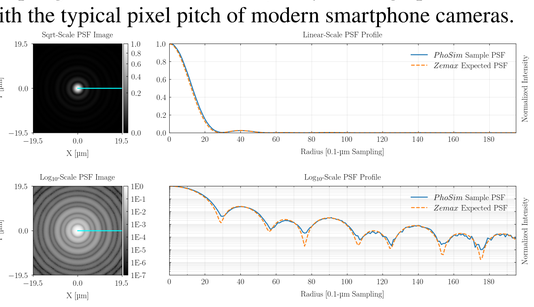

Fig. 6: *PhoSim*'s 1-μm PSF of FLUTE-1-A: even with relatively few photons, the diffraction fingerprint agrees with *Zemax*.

⟹ **See also col. *I* of the Biancalani+2026 AAS-247 iPoster and cols. *III* & *IV* of the Biancalani+2025 AAS-245 iPoster.**

The Quest for Avatar's Pandora at α Centauri & the Like

Modern astronomy started out with the observations that Galileo Galilei initiated in 1609 and published, in 1610, with his pamphlet entitled *Sidereus Nuncius* (meaning "Sidereal Messenger"). I.a., he discovered Jupiter's so-called "Galilean" moons.

In principle, the general-purpose Roman or Lazuli space telescopes have a chance at serendipitously detecting, via coronagraphic exoplanet-star relative astrometry, hypothetical exomoons down to some fraction of $M_\oplus$—similar to the fictional Avatar exomoon Pandora—around the habitable-zone Saturn-mass exoplanet candidate discovered (not yet confirmed) by Wagner+2021 at α Cen(tauri) *A*; see also the Beichman+2025 paper series. Such a discovery could revolutionize our understanding of exo-worlds and broaden the scope of larger missions like HWO in the search for alien life across our cosmic neighborhood. Even a partial or null detection could, perhaps, inform future intermediate-class FLUTE missions dedicated to continuous monitoring campaigns; which might benefit from consolidated technologies for multi-star systems (see, e.g., Thomas+2015, Sirbu+2017, or the upcoming TOLIMAN mission) and for astrometric calibration (see, e.g., Guyon+2012).

The following simulations by Kevin Wagner, based upon Wagner+2025, explore the performance parameter spaces of FLUTE and of the Nautilus Space Observatory—in parallel, see also the Wagner+2026 Nautilus White Paper—for indirectly detecting exomoons via the host exoplanet's orbital reflex motion.

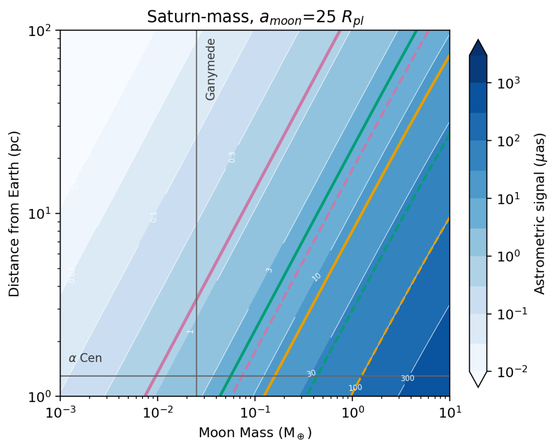

Fig. 7: Kevin Wagner's simulation mapping out the astrometric reflex signal (color bar) induced by a hypothetical exomoon on a Saturn-mass exoplanet, with a semi-major axis $a_{\rm moon}$ = 25 $R_{\rm pl}$, as a function of exomoon mass and distance to the host system. Color-coded detection-limit curves indicate single-aperture observatories with diameters of 3 m (orange), 8.5 m (green), and 50 m (purple). Dashed lines mark the single-epoch astrometric precision; solid lines mark a 5-year campaign floor.

⟹ **See also col. *II* of the Biancalani+2026 AAS-247 iPoster.**

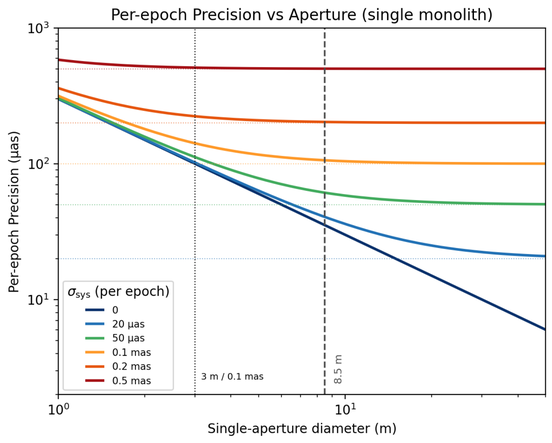

Fig. 8: Kevin Wagner's simulation investigating, for various regimes of systematic error, σ_{sys}, how the per-epoch astrometric precision scales with the effective primary diameter of FLUTE.

The following graph shows that, for coronagraphic astrometry, the science return of a single-aperture telescope is limited by systematics, unless these can somehow be calibrated out. On the other hand, the addition of telescope units to the Nautilus array can average down systematics, if these are independent across units, and augment the light-gathering power of the observatory—although its angular resolution does not improve.

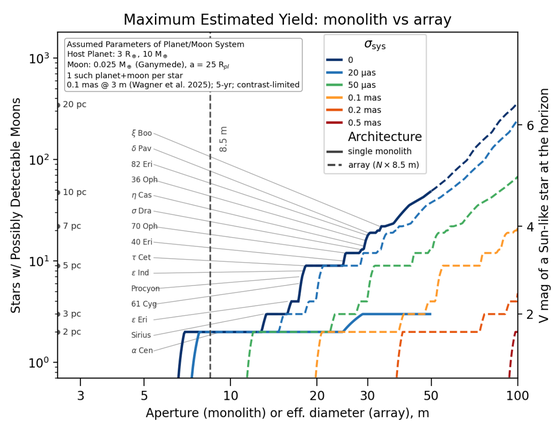

Fig. 9: Kevin Wagner's simulation of the maximum estimated number of stars—with corresponding survey-distance-horizon markers—that could host detectable exomoons, for FLUTE (solid lines) and for the non-interferometric Nautilus array (dashed lines), at various σ_{sys} levels. Here, FLUTE's effective diameter reaches up to 50 m; the effective diameter of the constellation of 8.5-m-diameter units constituting Nautilus reaches up to 100 m.

FLUTE Concept Variations on LUVOIR

The exoplanet discovery revolution is unfolding (almost) exponentially, with a doubling time of just few years, since the first confirmed detection of planets orbiting a star other than the Sun, in 1992, and of the first planet around a Sun-like star, in 1995.

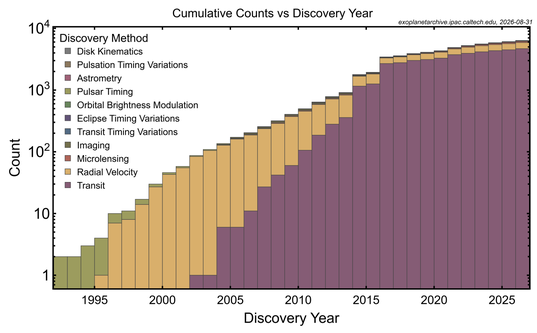

Fig. 10: NASA Exoplanet Archive's histogram of the cumulative count of exoplanets in time, color-coded by discovery method.

Although radial velocity and, then, transit have been the main contributing methods to the current census of confirmed exoplanets, direct high-contrast imaging and spectrography seem the most promising for seeking habitable or inhabited exo-Earths. According to Stark+2015b: "We conclude that a coronagraphic direct-imaging mission requires a >8.5 m aperture to provide a reasonable chance of finding an Earth-like planet." If the direct-characterization Large UV/Optical/IR (LUVOIR) Surveyor concept were to be revived, e.g., into a FLUTE mission with a ~12-m-aperture off-axis configuration, it could yield ~3 times the ~25 exo-Earth candidates recommended by the Decadal Survey on Astronomy and Astrophysics 2020 (Astro2020), over a 2-year blind-search survey. With an astro-photonic coronagraph, the yield multiplier could reach ~5×.

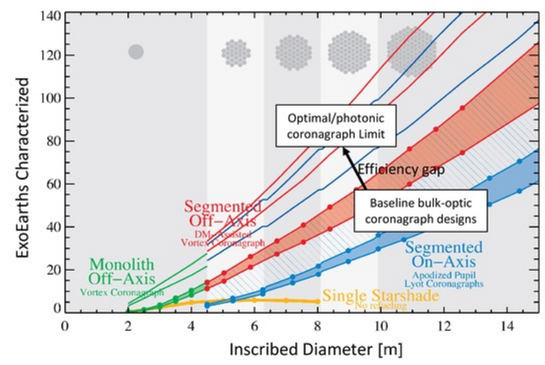

Fig. 11: Scaling graph, after Sirbu+2024, describing the theoretical impact of astro-photonics on the directly-imaged exo-Earth candidate yield (at optical wavelengths), as a function of the telescope's inscribed light-gathering aperture diameter.

Moreover, a fluidic telescope with a much larger diameter could be assembled to yield ~300 exo-Earth candidates, devoted to systematically searching for inhabited exo-Earths. Such a class of space telescope could be specialized in the characterization of potential bio-signatures or even techno-signatures—such as night-side city lights—on selected habitable exo-Earth targets. The upper critical bound of ~300 on the exo-Earth candidate yield can be estimated at the limit where overheads dominate over the observational time, independently of the diameter under study, adopting the following toy-model assumptions and approximations (C. Stark, personal communication):

- Let us consider a 2-year blind-search survey of stars supposed to host exoplanetary systems whereby all the observational time, corresponding to the total survey duration $t_{\rm tot} \sim 17,531.6$ hours, goes into overheads.
- With 7 (non-sequential) visits per star, the number of observable stars turns out to be (rounded down): $N_{\rm sys} = \dfrac{t_{\rm tot}}{(1\,{\rm hr}\times 6\,{\rm det.\ visits}) + (1\,{\rm hr}\times 1\,{\rm char.\ visit})} \cong 2504.$
- Under the assumptions that the scaling power laws do not really change in yield-diameter phase space and that the exo-Earth candidate occurrence rate[a] is $\eta_\oplus \equiv 0.24$, a 50% statistical survey completeness[b] leads to an exo-Earth candidate yield of ~300 (rounded down).

Given an underlying binomial distribution, according to the following formula by Stark+2014b, modified by Stark+2015b to include all exo-Earth candidates (ECs) in the statistics, this sample of ~300 ECs would allow the discovery of at least one exo-Earth with habitability tracers or bio-signatures at the $c \sim 99\%$ confidence level if the unconstrained statistical fraction of exo-Earths that exhibit spectral signatures characteristic of habitability or life (as we know it) is $f \gtrsim 1.5\%$ of all ECs. The probability of obtaining zero detections would be about 1%.

$$N_{\rm EC}\left\{\eta_\oplus, {\rm c}, f_{\rm (habitability\ or\ life)}\right\} = \eta_\oplus \frac{\log(1-c)}{\log(1-\eta_\oplus f)}.$$

This expression assumes that 100%-detectable signatures of habitability or life (as we know it) are present somewhere out there. For comparison, the sample of $N_{\rm EC} \sim 25$ recommended by the Astro2020 Decadal Survey would guarantee the discovery at the $c \sim 99\%$ confidence level of at least one habitable or inhabited exo-Earth only if $f \gtrsim 18\%$, i.e., if the minimum frequency of such exo-Earths is an order of magnitude higher than in the previous case. In other words, at any given frequency, the probability of mission success is roughly proportional to $N_{\rm EC}$.

[a] The exo-Earth candidate occurrence rate estimates the fraction of Sun-like stars with an exo-Earth candidate.

[b] Here, the statistical survey completeness indicates the average chance of a successful exo-Earth candidate observation if a given exo-Earth exists.

⟹ **See also col. *III* of the Biancalani+2026 AAS-247 iPoster and cols. *I* & *IV* of the Biancalani+2025 AAS-245 iPoster.**

Towards FLUTE-50 & Beyond

To put the status quo in perspective: we are currently living through a new space age, consisting of a new space economy and a race to the Moon, with the US leading the Artemis program. An instantiation of this era's *zeitgeist* is the season of space-based economy ushered in by *SpaceX*'s implementation and roll-out of rocket reusability—a partial reusability until *Starship* becomes operational—via vertical propulsive landing, in 2015, which essentially enabled an increased launch cadence. The graph below illustrates that the capability of launching objects beyond Earth's atmosphere is currently booming.

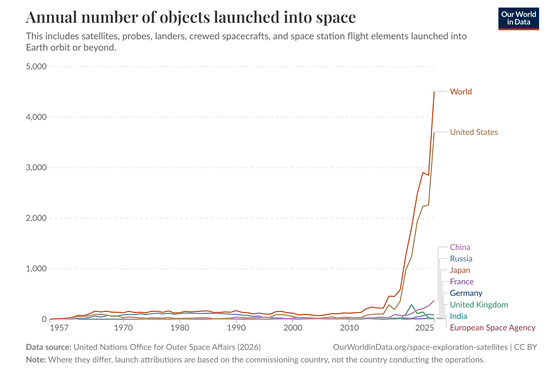

Fig. 12: Our World in Data: annual number of launched objects.

In the wake of this trend, FLUTE's approach has the potential of being a discovery leap enabler, by unleashing the benefits of space-assembled telescopes with much larger apertures than today's standard. In fact, the effective primary aperture of a telescope drives, i.a., angular resolution, light-gathering power (also affecting the spectral resolving power), and exposure time. The exposure time is a fundamental parameter both from an overall practical standpoint and, e.g., for capturing fast or diurnal exo-world cycles in their atmospheres or on their surfaces. To gauge its significance, we adapted Turyshev2026's direct-imaging toy model to get order-of-magnitude estimates of the exposure time as a function of the telescope's effective diameter.

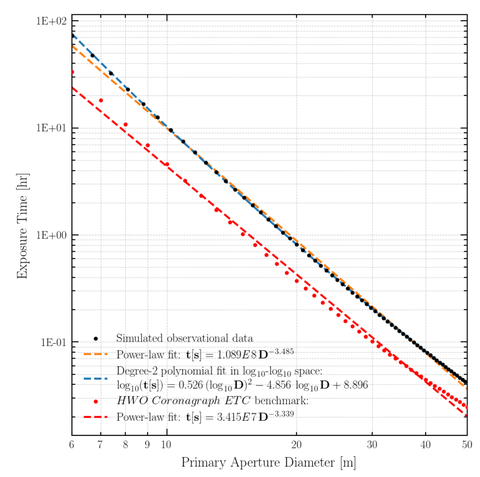

Fig. 13: Estimated exposure time vs diameter scaling for the direct imaging of an exo-Earth at 30 pc, following Turyshev2026.

HWO has baselined coronagraphs (left sketch, below) to suppress most of the starlight and directly search for habitable exoplanets. This operation will occur inside the telescope itself, which requires an ultra-stable adaptive coronagraphic system to minimize light speckles produced by the optics. However, starshades (right sketch, below) can relax this requirement by diffractively nulling most of the starlight before it enters the telescope. The price to pay is, literally, for an external occulter of (at least) tens of meters flying in formation with the telescope itself at separations of (at least) tens of thousands of kilometers.

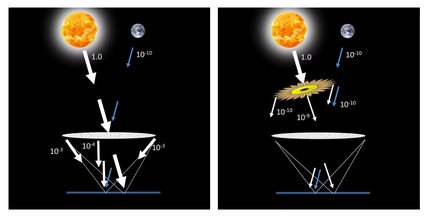

Fig. 14: Coronagraph (left) and starshade (right) operational principles for imaging an exo-Earth; from Project Starshade.

Starshades could be key to unlocking the direct characterization of "Galilean"-like moons around our nearest stars for classes of FLUTE with primary-aperture diameters of several tens of meters, such as FLUTE-50; see Biancalani+2025 for its preliminary optical design with an aspherical primary (FLUTE-50-A), traceable down to FLUTE-1-A and diffraction-limited at 1 μm over a circular FoV of ~0.8 arcminutes in diameter.

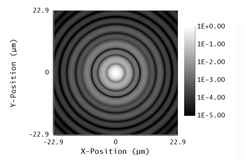

Fig. 15 (a): FLUTE-50-A's FFT 1-μm PSF, in *Zemax*.

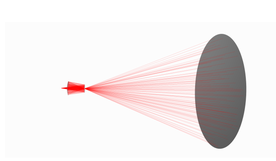

Fig. 15 (b): Optical design of FLUTE-50-A, in *PhoSim*.

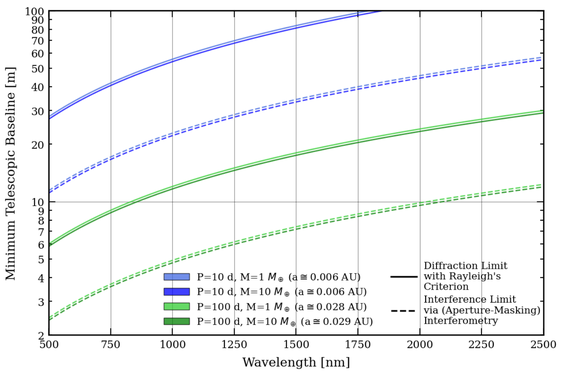

Fig. 16: Estimated minimum baseline, as a function of wavelength, necessary to angularly resolve a few sample hypothetical exomoon cases—in orbital period (P) and mass (M)—around a Saturn-mass exoplanet at α Cen *A*, with a single-aperture (monolithic) diffraction-limited telescope and with an interferometer (e.g., via sparse-aperture masking).

⟹ **See also col. *IV* of the Biancalani+2026 AAS-247 iPoster and cols. *I*, *III*, *IV* of the Biancalani+2025 AAS-245 iPoster.**

Main References: Biancalani+2026 | Macro-Evolution-Telescopes GitHub repo. | STScI 2025 Annual Report | Bercovici Fluidic Technologies Lab's pubs. | Biancalani+2025 | *PhoSim* website | Wagner+2021 | Wagner+2025 | NASA Exoplanet Archive | Decadal Survey on Astronomy and Astrophysics 2020 (Astro2020) | Sirbu+2024 | Stark+2015b | Our World in Data website | Turyshev2026 | Project Starshade